Catalysis
Science &
Technology

Reduced graphene-tungsten trioxide-based hybrid materials with peroxidase-like activity

SCHOLARONE™
Manuscripts

Catalysis Science & Technology

COMMUNICATION

Reduced graphene-tungsten trioxide-based hybrid materials with peroxidase-like activity

Chenbo Dong,[a#] Alixandra Wagner,[a#] Valentina Dinca,[b] and Cerasela Zoica Dinu[a]*

A hybrid was synthesized using tungsten trioxide and graphene as starting materials. Hybrid's characteristics were investigated by scanning and transmission microscopy, Raman and adsorption spectroscopy. Incubation with model chemical compound used for evaluating oxidative degradation showed enzymatic-like activity. Future application for decontamination-based platforms is envisioned.

Aqueous effluents resulted during coal-conversion have been shown to contain high concentrations of phenolic compounds.[1,2] Toxicity of such compounds range from 9 to 25 mg/L[3] and could produce respiratory anomalies in humans as result of both lung and mucous membrane irritations,[4,5] and/or irritation of the gastrointestinal and central nervous systems.[5] Complementary, in aquatic life, phenolic compounds contamination was shown to lead to both changes of the ecosystem[6,7] as well as metabolic changes in fish populations.[8,9] Considering that half-lives for degradation of phenolic compounds range from days to months,[10] depending on the source of pollution and the location of the pollutant itself (i.e., in the wastewater of the lakes or rivers or in the estuarine water),[11] a variety of hazard mitigation strategies have been developed to eliminate such compounds. Current methods rely on distillation,[12] solid-phase or liquid-liquid extractions,[13] photo-oxidation,[14] or membrane treatments.[15] While somewhat effective, such methods are not economically feasible since they require a large amount of energy investment. Further, studies showed that such methods might need selective reactors to help achieve high efficiency of contaminant removal.[16] Lastly, analysis showed that if for instance membranes are used, strategies aimed at reducing fouling and pore wetting/clogging need to be implemented.[17]

Enzyme-based treatments have been applied as inexpensive means for transforming phenolic compounds into user and environmentally friendly products.[18] Studies showed that soybean and horseradish peroxidases for instance are two of the most common enzymes used in the removal of such organic pollutants especially the ones resulted from industrial wastewater.[19] Studies by Yu et al., showed that horseradish peroxidase removed 95 % of phenol (188 mg/mL) producing five dimeric and one trimeric products.[20] Additionally, Gómez et al., showed that 80 % of the phenol was removed with derivatives of soybean peroxidase immobilized onto glass supports.[21] Complementary, Zhang et al., immobilized horseradish peroxidases on graphene oxide and showed that such hybrids could lead to 88 % phenol removal.[18] Finally, Caza et al., found that changing the pH or adding polyethylene glycol to an enzymatic system based on peroxidases could increase the efficiency of decontamination by up to 95 %.[22] However, while such enzyme-based decontamination has proven highly effective, approaches to increase enzyme's operational stability need to be developed and implemented in order to achieve industrially feasible decontamination. Ideally, the next strategy should be synthetic, easy to design and implement, and demonstrate high efficiency of decontamination while possessing long lasting shelf life, stability and reusability characteristics that reduce logistical burdens to environment or user.

"Smart" materials have recently been proposed as alternatives capable to mimic the natural specificity and selectivity of biological catalysts. Called "nanozymes" or "artificial enzymes",[23] such materials were developed to ensure a biological-like function is implemented to a non-biological material. By mimicking the architecture of the catalase enzyme for instance, semiconductor materials such as titanium dioxide (TiO_2) were shown to display excellent catalytic capability.[24] Unique properties such as surface area or conductivity have been optimized to increase materials' potentials for acting as natural catalysts in a variety of pH's or temperature conditions.[25] In water for instance, study showed efficient removal of organic pollutants when TiO_2 materials with enzyme-like activity have been used; further, such materials demonstrated high stability and long operation times.[26]

a. Department of Chemical and Biomedical Engineering, West Virginia University, Morgantown, WV, 26506

b. National Institute for Lasers, Plasma and Radiation Physics, 409 Atomistilor Street, Magurele, 077125, Romania

#The authors have contributed equally to this publication.

This journal is © The Royal Society of Chemistry 2018

Catal. Sci. Technol, 2018, **00**, 1-3 | **1**

COMMUNICATION

Nevertheless, the relative large band gap of the TiO_2-based materials, the high recombination rate of photo-generated electron-hole pairs, the usually UV restricted activity, non-specificity of detection, and aggregation in certain solutions, were shown to limit their consumer implementation.[27,28] If nanozymes are to be exploited for decontamination purposes, then alternative strategies aimed to ensure high efficiency in a wide range of light spectra need to be considered. Herein we propose to create the next generation of nanozymes with peroxidase-like activity. Our approach combines tungsten trioxide (WO_3), a material capable of utilizing visible light for its activity[29,30] and graphene, a material that allows faster charge transfer at its interface,[31] to develop hybrids. Such hybrid was formed through mechanical stirring of WO_3 and reduced graphene oxide (r-GO); photodecomposition of Pt was also used to increase multi-electron O_2 reduction at the hybrid interface[32] (**Scheme 1**).

Hybrids' physicochemical characterization was performed via scanning electron microscopy (SEM), high-resolution transmission electron microscopy (TEM), Raman and adsorption spectroscopy respectively. SEM analyses revealed that the hybrids exhibited mixed geometries consisting of larger and smaller particles of irregular shapes (**Figure 1a**). The observed geometries resembled the ones of controls WO_3 (**Figure 1b**) or Pt-WO_3 (**Figure 1c**), with more fragmented aspect ratios being observed for the Pt-WO_3 relative to WO_3. This was presumably due to the additional preparation step required, i.e., that of Pt photodeposition. Control r-GO exhibited a layered sheet-like geometry (**Figure 1d**). Our morphology analysis are supported by previous reports and confirm both the controls' physical geometries as well as the characteristics of the hybrid being formed.[32] High-resolution TEM confirmed the crystalline lattice spacing of the core materials in the hybrid. Specifically, analysis showed that the bulk WO_3 had a crystalline lattice spacing of about 0.38 nm that was previously correlated with the (020) plane (**Figure 2a**).[32] Pt photodeposition led to small nanoparticles (diameters from 5 to 20 nm) formation, with such particles bulking of WO_3. Further, such nanoparticles had an inter-planar spacing of 0.23 nm as identified by the (111) lattice plane of Pt (**Figure 2b**). Our analysis have also showed that Pt was non-uniformly distributed at the contact interface with the WO_3 most likely due to Pt's inclination to deposit and interact at the small facets/edges such as the ones corresponding to the (020) crystalline planes.
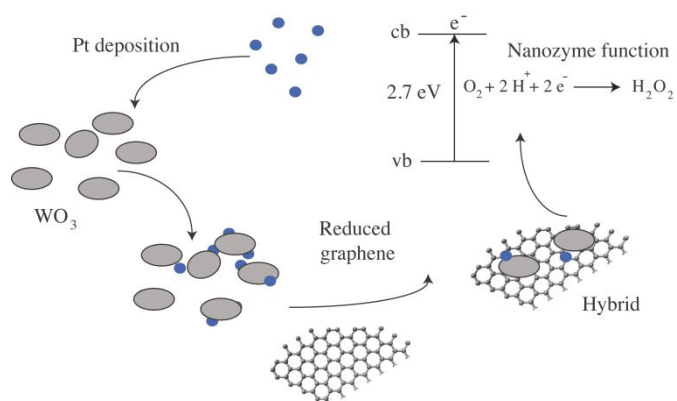
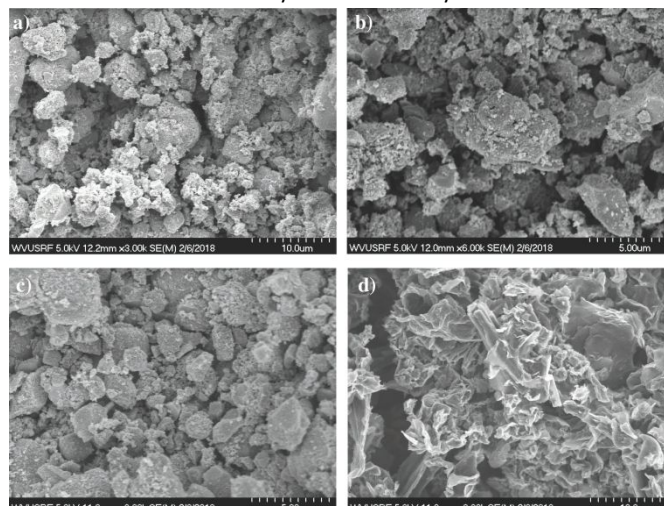**Scheme 1:** Formation of a hybrid with nanozyme function.

Figure 1: Scanning electron microscopy (SEM) images of hybrids (a), and controls WO_3 (b), Pt-WO_3 (c) and r-GO (d) respectively.

Raman spectroscopy allowed hybrids' chemical characterization. Specifically, sample analysis (**Figure 2c**) identified peaks around 810 cm^{-1} and 710 cm^{-1} attributed to the stretching of the O–W-O bonds, as well as peaks at 328 cm^{-1} and 270 cm^{-1} respectively, related to the bending vibration of the W–O-W bonds. Peaks below 200 cm^{-1} were associated with the vibrations of the WO_3 lattice modes. Comparisons with r-GO starting material used as control, identified a D peak at 1349 cm^{-1} for the Pt-WO3-r-GO which was shifted from the initial 1356 cm^{-1}, presumably indicating an increase in the size of in-plane sp2 structure domains and/ or a disorder in the C structure resulted from the reduction process. Similarly, a G peak shifted from 1594 to 1598 cm^{-1} was identified for the Pt-WO3-r-GO, possibly because of the sp2 C vibration. The relative intensity (I) of D to G peaks (an indicator of the disorder degree in the C-based hybrids) was 0.94 for the Pt-WO_3-r-GO relative to the r-GO (0.83) used as control. The increase in I_D/I_G ratio indicated the higher disorder associated with the sp2 bonds and possible structural defects in the hybrids.

WO_3 and Pt-WO_3-r-GO displayed similar patterns of absorption in the UV range of light (range 200-800 nm; **Figure 2d**). Further, Pt-WO_3-r-GO showed an increase in adsorption in the visible region. This could be presumably due to the improved photoactivity of the hybrid as resulted from the incorporation of r-GO even at the low concentration of 2% being used in our experiments. In particular, previous research has showed that r-GO could increase the electron transfer from the conduction band of WO_3 to contribute to enhanced photoactivity.[32] Our results are similar to previously reported.[33,34,35] Irie et al., for instance, showed an increase in absorbance at 460 nm, which was attributed to the 2.7 eV band gap of WO_3.[34] Complementary, Aslam et al., examined the effects of modifying WO_3 with metal ions and found that increasing the loading wt. % through addition of Ag^+ also increased the absorbance in the visible region. [33]

2 *Catal. Sci. Technol*, 2018, **00**, 1-3

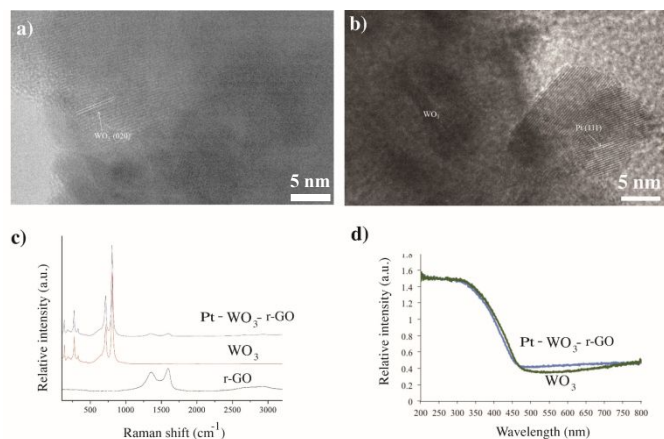This journal is © The Royal Society of Chemistry 2018

Figure 2: a) High-resolution transmission electron microscopy (TEM) of WO_3 showing the crystalline lattice spacing correlated with the (020) plane. b) TEM of Pt-WO_3 showing an inter-planar spacing of 0.23 nm identified as the (111) lattice plane of Pt. c) Raman spectroscopy of the Pt-WO_3-r-GO hybrids. d) UV-VIS spectroscopy analysis of WO_3 and Pt-WO_3-r-GO.

To demonstrate that the created hybrid could serve as a nanozyme that possess peroxidase-like activity, we monitored the oxidative coloration of model chemical compound, 2,2'-azino-bis(3-ethylbenzothiazoline-6-sulphonic acid) (ABTS; **Figure 3a**). Previous research has showed that ABTS could be catalyzed by natural peroxidases in the presence of hydrogen peroxide (H_2O_2) with such catalysis to result in a color change recorded in visible light, i.e., at 415 nm.[36] Our hypothesis was that the user-synthesized hybrid incubated with ABTS would be able to generate reactive oxygen species (peroxide for instance) under light irradiation to thus lead to spectroscopic transformation of the reagent. The hypothesis was based on previous results which showed that an enhanced photocatalytic ability could be achieved for such hybrids due to the existing strong coupling between the Pt-WO_3 and r-GO surfaces, with such coupling to promote interfacial electron transfers and increase the rates of recombination.[37]
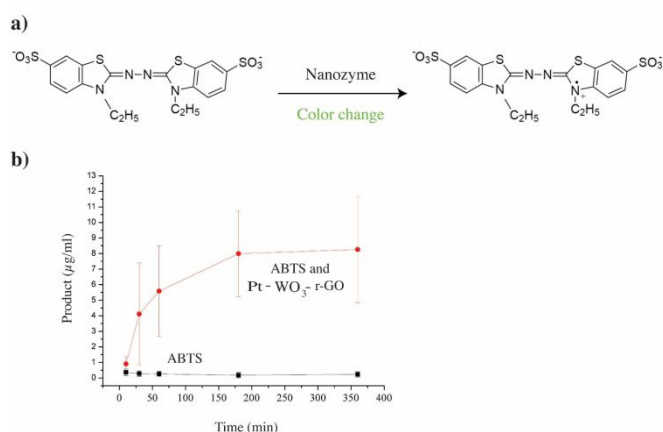

Figure 3: a) Oxidative coloration of model chemical compound, 2,2'-azino-bis(3-ethylbenzothiazoline-6-sulphonic acid) (ABTS) under the reactive oxygen species generated by the hybrid. b) ABTS oxidation converted through the Beer–Lambert law.
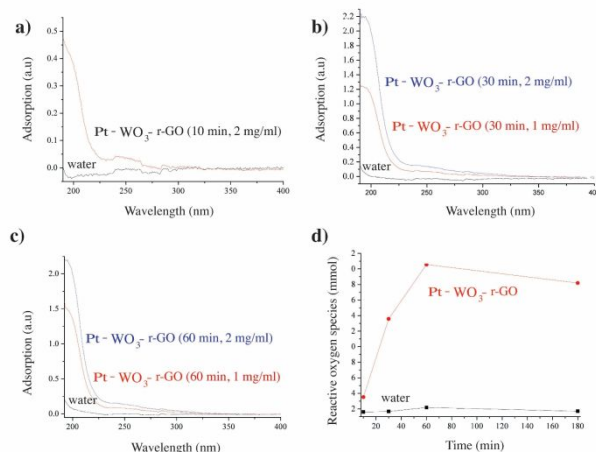

Figure 4: a) Reactive oxygen species generated by the hybrid irradiated for 10 min (a), 30 min (b) and 60 min (c) respectively. d) Reactive oxygen species converted into the absorption data using the Beer–Lambert law.

Indeed, our analysis (as converted through the Beer–Lambert law) showed ABTS oxidation upon incubation of the reagent with the hybrids, all under visible light (**Figure 3b**). Specifically, results revealed that the addition of the hybrid leads to changes in the reagent coloration only after 30 min observation time, with the full oxidation of ABTS reaching a saturation level after about 3 h incubation. No oxidative change was observed when control ABTS (reagent without hybrid) was placed under visible light irradiation. Complementary, when hybrids were dispersed in Di water and subsequently irradiated under visible light for different time intervals, their adsorption intensity in the 190 to 400 cm^{-1} increased with the irradiation time (**Figure 4 a-c**). Further, in the 190-350 nm region, the absorption cross-section increased monotonously as the wavelength decreased, allowing for reactive oxygen species to be quantified[38] by converting the absorption data using the Beer–Lambert law (**Figure 4d**).

Our results are supported by previous studies that showed that adsorption is correlated with reactive oxygen species generation,[39] with studies indicating that hydrogen peroxide for instance absorbs light at wavelengths shorter than 350 nm. It should be noted that some of the reactive oxygen species that were possibly generated herein may also dissolve in the solution during the experimental set up being used, thus leading to lower quantified adsorption levels. This assumption is supported by previous research that showed that at wavelength higher than 193 nm the only stable photolysis product of peroxide is the OH radical.

We have demonstrated that hybrid materials based on WO_3 have peroxidase-like activity in visible light. Our approach provides a reliable colorimetric method for model compound oxidation identification as well as evaluation of reactive oxygen species generation only after 10 min of light exposure. Such design strategy could be implemented in the development of the next platforms to be used for decontamination of phenolic products with a high activity and operational stability. Further, knowing that WO_3 could

detect gases and trace pollutants while acting as an electrochromic material with cyclic durability,[40] and based on graphene's capability to enhance chemical coupling as well as to provide enhanced energy storage and increased cyclic stability,[41,42] we envision extending our approach to demonstrate hybrid's ability for organic dye adsorptivity and degradation.
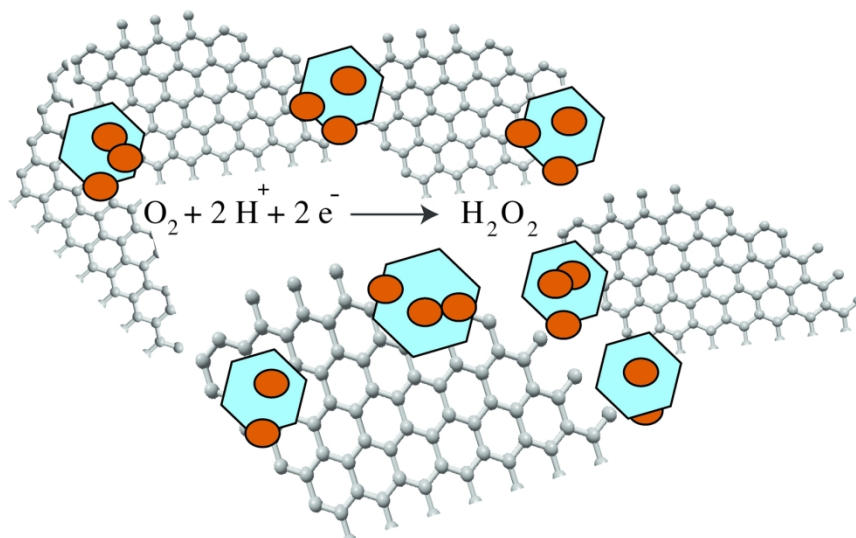
Conflicts of interest
There are no conflicts of interest to declare.

Notes and references

1   V. L. Santos and V. R. Linardi, *Process Biochem.*, 2004, **39**, 1001 1006.
2   M. A. Zazouli and M. Taghavi, *Journal of Water Resources and Protection*, 2012, **4**, 980-983.
3   S. J. Kulkarni and J. P. Kaware, *Int. J. Sci. Res.*, 2013, **3**.
4   U. S. N. L. o. Medicine, *Journal*, 2003.
5   J. Michalowicz and W. Duda, *Pol. J. Environ. Stud.*, 2007, **16**, 347-362.
6   A. L. Buikema, M. J. McGinniss and J. Cairns, *Mar. Environ. Res.*, 1979, 87-181.
7   N. C. Saha, F. Bhunia and A. Kaviraj, *Bull. Environ. Contam. Toxicol.*, 1999, **63**, 195-202.
8   S. Gupta, R. C. Dalela and P. K. Saxena, *Environ. Res.*, 1983, **32**, 8-13.
9   A. L. van Boxtel, J. H. Kamstra, P. H. Cenijin, B. Pieterse, J. M. Wagner, M. Antink, K. Krab, B. van der Burg, G. Marsh, A. Brouwer and J. Legler, *Environ. Sci. Technol.*, 2008, **42**, 1773-1779.
10 H. M. Hwang, R. E. Hodson and R. F. Lee, *Photochemistry of Environmental Aquatic Systems*, 1987, **327**, 27-43.
11 G. Ying, B. Williams and R. Kookana, *Environ. Int.*, 2002, **28**, 215-226.
12 V. Janda and K. Krijt, *J. Chromatogr.*, 1984, **283**, 309-314.
13 C. Mahugo Santana, Z. Sosa Ferrera, M. Esther Torres Padron and J. Juan Santana Rodriguez, *Molecules*, 2009, **14**, 298-320.
14 S. Azabou, W. Najjar, A. Gargoubi, A. Ghorbel and S. Sayadi, *Appl. Catal. B.*, 2007, **77**, 166-174.
15 H. Kiai, M. C. García-Payo, A. Hafidi and M. Khayet, *Chemical Engineering and Processing: Process Intensification*, 2014, **86**, 153-161.
16 G. Busca, S. Berardinelli, C. Resini and L. Arrighi, *J. Hazard. Mater.*, 2008, **160**, 265-288.
17 M. Laqbaqbi, J. A. Sanmartino, M. Khayet, C. García-Payo and M. Chaouch, *Applied Sciences*, 2017, **7**.
18 F. Zhang, B. Zheng, J. Zhang, X. Huang, H. Liu, S. Guo and J. Zhang, *J. Phys. Chem. C*, 2010, **114**, 8469-8473.
19 N. Durán and E. Esposito, *Appl. Catal.*, 2000, **28**, 83-99.
20 J. Yu, K. E. Taylor, H. Zou, N. Biswas and J. K. Bewtra, *Environ. Sci. Technol.*, 1994, **28**, 2154-2160.
21 J. L. G´omez, A. B´odalo, E. G´omez, A. M. Hidalgo, M. G´omez and M. D. Murcia, *Chemical Engineering Journal*, 2007, **127**, 47-57.
22 N. Caza, J. K. Bewtra, N. Biswas and K. E. Taylor, *Water Res.*, 1999, **33**, 3012-3018.
23 X. Hu, J. Liu, S. Hou, T. Wen, W. Liu, K. Zhang, W. He, Y. Ji, H. Ren, Q. Wang and X. Wu, *Science China Physics, Mechanics and Astronomy*, 2011, **54**, 1749-1756.
24 A. Truppi, F. Petronella, T. Placido, M. Striccoli, A. Agostiano, M. Curri and R. Comparelli, *Catalysts*, 2017, **7**, 100.
25 M. Drozd, M. Pietrzak, P. Parzuchowski, M. Mazurkiewicz-Pawlicka and E. Malinowska, *Nanotech.*, 2015, **26**.
26 J. Mu, J. Li, X. Zhao, E. Yang and X. Zhao, *RSC Adv.*, 2016, **6**.
27 S. A. Ansari and M. H. Cho, *Sci. Rep.*, 2016, **6**.
28 X. Wang, T. Li, R. Yu, H. Yu and J. Yu, *J. Mater. Chem. A*, 2016, **4**.
29 Y. Wicaksana, S. Liu, J. Scott and R. Amal, *Molecules*, 2014, **19**, 17747-17762.
30 S. K. Gullapalli, R. S. Vemuri and C. V. Ramana, *Appl. Phys. Lett.*, 2010, **96**.
31 M. Pan, Y. Zhang, C. Shan, X. Zhang, G. Gao and B. Pan, *Environ. Sci. Technol.*, 2017, **51**, 8597-8605.
32 C. Dong, R. Eldawud, A. Wagner and C. Z. Dinu, *Appl. Catal. A*, 2016, **524**, 77-84.
33 M. Aslam, M. Tahir Soomro, I. M. I. Ismail, N. Salah, M. Waqar Ashraf, H. A. Qari and A. Hameed, *Arabian Journal of Chemistry*, 2015, DOI: 10.1016/j.arabjc.2015.05.001.
34 H. Irie, H. Miura, K. Kamiya and K. Hashimoto, *Chem. Phys. Lett.*, 2008, **457**, 202-205.
35 P. M. Rao, L. Cai, C. Liu, I. S. Cho, C. H. Lee, J. M. Weisse, P. Yang and X. Zheng, *Nano Lett.*, 2014, **14**, 1099-1105.
36 A. S. Campbell, C. Dong, F. Meng, J. Hardinger, G. Perhinschi, N. Wu and C. Z. Dinu, *ACS Appl. Mater. Interfaces*, 2014, **6**, 5393-5403.
37 Y. Y. Liang, H. L. Wang, H. S. Casalongue, Z. Chen and H. J. Dai, *Nano Res.*, 2010, **3**, 701-705.
38 A. Hofmann, *Principles and Techniques of Biochemistry and Molecular Biology*, 2010, 477-521.
39 S. P. Sander, R. R. Friedl, D. M. Golden, M. J. Kurylo, R. E. Huie, V. L. Orkin, G. K. Moortgat, A. R. Ravishankara, C. E. Kolb, M. J. Molina and B. J. Finlayson-Pitts, *JPL Publications*, 2003, **Evaluation No. 14**, 02-25.
40 A. Subrahmanyam and A. Karuppasamy, *Sol. Energy Mater. Sol. Cells*, 2007, **91**, 266-274.
41 R. Kumar, R. K. Singh, A. V. Alaferdov and S. A. Moshkalev, *Electrochim. Acta,* 2018, **281**, 78-87.
42 R. Kumar, E. Joanni, R. K. Singh, D. P. Singh and S. A. Moshkalev, *Prog. Energy Combust. Sci.,* 2018, **67**, 115-157.

4 *Catal. Sci. Technol*, 2018, **00**, 1-3

This journal is © The Royal Society of Chemistry 2018

$$O_2 + 2\,H^+ + 2\,e^- \longrightarrow H_2O_2$$

Hybrid material with enzyme-like function

164x127mm (300 x 300 DPI)